Indian Journal of Chemistry
Vol. 59A, February 2020, pp. 189-199

Photochromic behaviour of Copper(I) and Silver (I) complexes of 1-alkyl-2-(arylazo)imidazoles in miceller media

B Chowdhury[a], D Mallick[b,] *, K K Sarkar[c], C Sen[d] & C Sinha[a,] *

[a]Department of Chemistry, Jadavpur University, Kolkata, West Bengal 700 032, India
[b]Department of Chemistry, Mrinalini Datta Mahavidyapith, Kolkata, West Bengal 700 051, India
[c]Department of Chemistry, Mahadevananda Mahavidyalaya, Kolkata, West Bengal 700 120, India
[d]Department of Chemistry, Sripat Singh College, Jiaganj, Murshidabad, West Bengal 742 123, India

Email: crsjuchem@gmail.com (C S)/ dmchemmdm51@gmail.com (D M)

Received 23 October 2018; revised and accepted 16 January 2020

Photochromism, a fast reversible structural change even at less than a femto second order upon irradiation of light, is largely influenced by the environment such as, polarity of media, existence of non-covalent interactions, hydrogen bonding etc. In this work, the micelle environment has been imposed on $[Cu(RaaiR')_2]ClO_4$ and $[Ag(RaaiR')_2]NO_3$ (RaaiR' = 1-alkyl-2-(arylazo)imidazole) in MeOH solution using Triton-X-100 (CMC, 108 ± 1.16 at 298 K), CTAB (CMC, 51.64 ± 1.04 at 298 K) and SDS (CMC, 207.01 ± 1.51 at 298 K). 1-alkyl-2-(arylazo)imidazole undergoes *trans*-to-*cis* and *vice-versa* isomerization about –N=N- bond upon light irradiation. The quantum yield ($\phi_{t\rightarrow c}$) of the photoisomerization follows the order - nonionic micelle (Triton-X-100) > Cationic micelle (CTAB) > no micelle > anionic micelle (SDS). The *cis*-to-*trans* isomerization is a thermally induced process. The activation energy of *cis*-to-*trans* isomerization is calculated by controlled temperature (298–313 K) experiment. Triton-X-100 and CTAB amplify the activation energy of *cis* → *trans* thermal isomerization while SDS reduces it.

Keywords: 1-Alkyl-2-(arylazo)imidazoles, Cu(I) and Ag(I) complexes, Photoisomerisation, Effects of micelle

Various external stimuli like thermal, magnetic, mechanical, electrical, redox, light activate molecules have been used for molecular switches. The reversible control of physical or chemical properties at the molecular level becomes a challenge in the field of designing molecular machines[1-4]. Light offers an attractive trigger and has enormous advantages over other activation processes[5]. Irradiation of light on azobenzene derivatives influences the structural change very fast between *trans* and *cis* isomers[6-9]. For the last few years we have been using light as stimulus to follow the *trans*-to-*cis* isomerization of arylazoimidazole (Scheme 1) and their metal complexes[10-17]. To explain the molecular mechanism of the *trans*-to-*cis* conversion[18] and the effect of crowded environment in solution of different solvent properties (density, polarity, viscosity, hydrogen bonding ability, vanderWaals, electrostatic activity etc.) and in the presence of noninteracting (innocent) and interacting (noninnocent) foreign molecules an exhaustive workup is necessary.

We have taken an effort to account the effect of different parameters (physical and chemical) on the photochromism of coordinated 1-alkyl-2-(arylazo)imidazoles in $[M(RaaiR')_2]^+$. This article concerns the effect of microenvironment augmented by adding micelle in solution on the photo-isomerisation of coordinated arylazoimidazoles. Self-assembly of micelles by aggregation in liquid influences the change in analyte concentration at the surface phase compared to bulk. Formation of hydrophobic core may increase concentration of organic molecules which certainly change physicochemical properties of the concerned

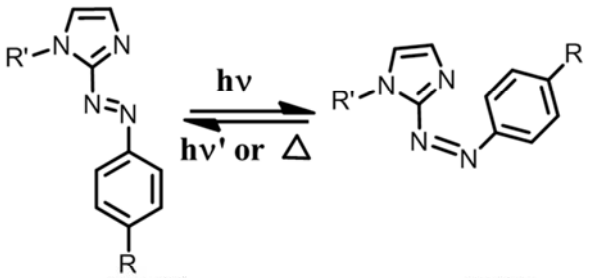

trans- (Z) *cis*- (E)
Isomerization of 1-alkyl-2-(arylazo)imidazole (ν > ν').
Scheme 1

system. In this work, we use SDS, CTAB and Triton-X 100 in methanol medium for the examination of photochromism of coordinated 1-alkyl-2-(arylazo)imidazoles in the complexes, $[M(RaaiR')_2]^+$ (M = Cu(I), Ag(I)).

Materials and Methods

Reagents/ Materials

1-alkyl-2-(arylazo)imidazoles and $[Cu(RaaiR')_2](ClO_4)$, $[Ag(RaaiR')_2](NO_3)$ complexes were synthesized by reported procedure[17]. Imidazole, aniline and *p*-toluidine were of analytical reagent grade received from SRL, India. SDS (Sodium dodecyl sulfate), Cetyl-(trimethyl)ammonium bromide (CTAB) and Triton-X were purchased from Sigma-Aldrich. All other chemicals and solvents were reagent grade as received.

Physical measurements

Spectroscopic data were obtained using the following instruments: UV-visible spectra from Perkin Elmer Lambda 25 spectrophotometer, photo-excitation has been carried out using Perkin Elmer LS-55 spectrofluorimeter. The mass spectra of the compounds were collected from a Water HRMS spectrometer (XEVO-G2QTOF#YCA351).

Photometric measurements

Absorption spectra were taken with a Perkin Elmer Lambda 25 UV-visible Spectrophotometer in a 1×1 cm quartz optical cell maintained at 25 °C. The light source of a Perkin Elmer LS 55 spectrofluorimeter was used as an excitation light, with a slit width of 10 nm. An optical filter was used to cut off overtones when necessary. The absorption spectra of the *cis* isomers were obtained by extrapolation of the absorption spectra of a *cis*-rich mixture for which the composition is known from ^{1}H NMR integration. Quantum yields (ϕ) were obtained by measuring initial *trans*-to-*cis* isomerisation rates (ν) in a well-stirred solution within the above instrument using the equation:

$$\nu = (\phi\, I_0 / V)(1 - 10^{-Abs}) \quad \ldots (1)$$

Where I_0 is the photon flux at the front of the cell, V is the volume of the solution, and Abs is the initial absorbance of azobenzene (ϕ = 0.11 for π-π* excitation[19,20]) under the same irradiation condition.

Computational methods

The geometry optimization of the complexes $[Cu(MeaaiMe)_2]^+$ (**1b**) and $[Ag(MeaaiMe)_2]^+$ (**3b**) were carried out using density functional theory (DFT) at the B3LYP level[21]. All calculations were carried out using the Gaussian 03 program package[22] with the aid of the Gauss View visualization program[23]. For C, H, N and O the 6-31G (d) basis set were assigned, while for Cu/Ag the LANL2DZ basis set with effective core potential was employed[24]. The vibrational frequency calculations were performed to ensure that the optimized geometries represent the local minima and there are only positive eigenvalues. Vertical electronic excitations based on B3LYP optimized geometries were computed using the time-dependent density functional theory (TD-DFT) formalism[25-27] in acetonitrile using conductor-like polarizable continuum model (CPCM)[28]. Gaus Sum was used to calculate the fractional contributions of various groups to each molecular orbital[29].

Results and Discussion

1-Alkyl-2-(arylazo)imidazole is a suitable bidentate chelating N(imidazolyl), N(azo) ligand[12-17] and forms Cu(I), $[Cu(RaaiR')_2]ClO_4$ and Ag(I), $[Ag(RaaiR')_2]NO_3$ complexes (Scheme 2). The complexes are characterized by spectroscopic data and the structural confirmation has been achieved in some cases by single crystal X-ray diffraction data[30-32]. ESI-MS shows Molecular ion peak at 463.0198 for $[Cu(Meaai\text{-}Me)_2]^+$ (**1b**) (m/z (calc.), 463.1420) and mass spectrum of $[Ag(Meaai\text{-}Me)_2]^+$ (**3b**) complex shows at 507.1981; (m/z (calc.), 507.1175) (Supplementary Data, Figs. S1 and S2).

The absorption spectra of the complexes are recorded in MeOH in 200–900 nm. The spectra show the absorption band around 370–390 nm with a molar absorption coefficient on the order of 10^4 M^{-1} cm^{-1} which corresponds to π-π* transitions and a weak tail

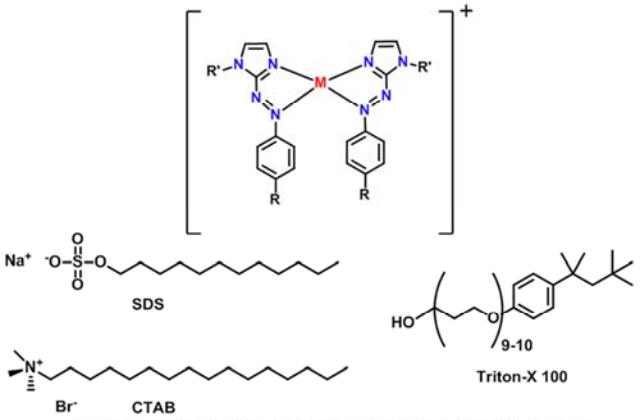

[M = Cu(I), [Cu(RaaiR')2]ClO4 (1, 2); M = Ag(I), [Ag(RaaiR')2]NO3 (3, 4)
R = H, R' = Me (1a), R = Me, R' = Me (1b); R = H, R' = Et (2a), R = Me, R' = Et (2b);
R = H, R' = Me (3a), R = Me, R' = Me (3b); R = H, R' = Et (4a), R = Me, R' = Et (4b)].

Scheme 2

covering to 450 nm refers to a n-π* transition[10,19,33]. Irradiation of methanol solution of the complexes with UV light in presence of Triton-X-100, CTAB and SDS changes the absorption spectrum as shown in Fig. 1. Fluorescence method is employed to determine critical micelle concentration (CMC) of the micelles in MeOH and data are (CMC at 298 K: Triton-X-100, 108 ± 1.16; CTAB, 51.64 ± 1.04 and SDS, 207.01 ± 1.51) in the acceptable range[34]. The intense absorption peak at 380 nm decreases accompanied by a slight increase at the longer wavelength portion of the spectrum at 490 nm until a stationary state is reached. Subsequent irradiation at the newly appeared longer wavelength peak reverses the course of the reaction and the original spectrum is recovered up to a point, which is another photostationary state under irradiation at the longer wavelength peak. The quantum yields of the *trans*-to-*cis* photoisomerization were determined using those of azobenzene as a standard and the results are tabulated in Table 1.

Upon irradiation with UV light *trans*-to-*cis* photoisomerisation of RaaiR' in methanol proceeds and the *cis* molar ratio reaches to >95%. The absorption spectra of the *trans*-ligands change with isosbestic points upon excitation (Fig. 2) into the *cis*-isomer. The ^{1}H NMR technique has been adopted to measure the percentage composition of the irradiated solution which supports the composition obtained from absorption spectra. The ^{1}H NMR signals of the aromatic ring protons are significantly shifted to upper field portion after the light irradiation. The quantum yields for the *trans*-to-*cis* ($\phi_{t\rightarrow c}$) photoisomerisation of these compounds in methanol in presence of Triton-X-100, CTAB and SDS on irradiation with UV light (Table 1) are significantly dependent on nature of substituents. Subtle increase in mass of the photochrome influences the rate and quantum yield of photoprocess; the Me substituent at azophenyl group (Haai-R to Meaai-R) and Et substituent at N(1)-position (1-Me to 1-Et) both reduce $\phi_{t\rightarrow c}$ values. In general, increase in mass

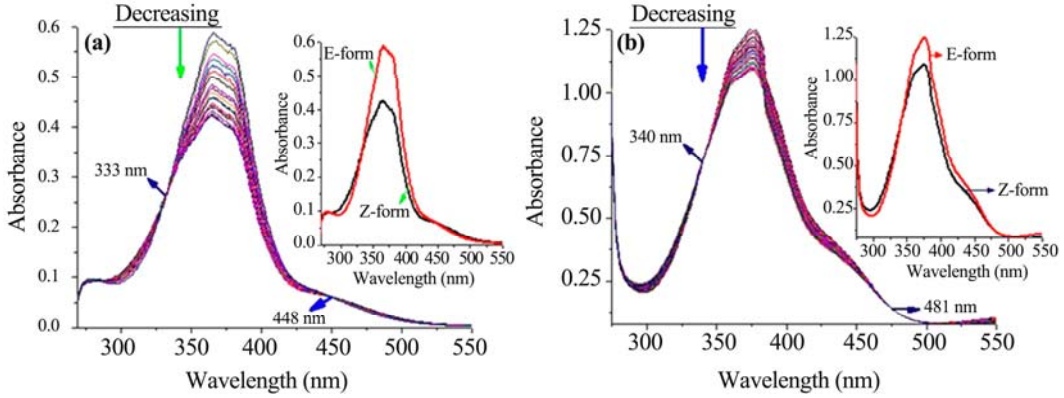

Fig. 1 — (a) Spectral changes of $[Cu(Meaai\text{-}Me)_2](ClO_4)$ in MeOH and (b) MeOH in presence of CTAB(1:1) upon repeated irradiation at 366 nm at 5 min interval at 25 °C; Inset: Z-form (*cis)* and E-form (*trans)* isomer of the complex.

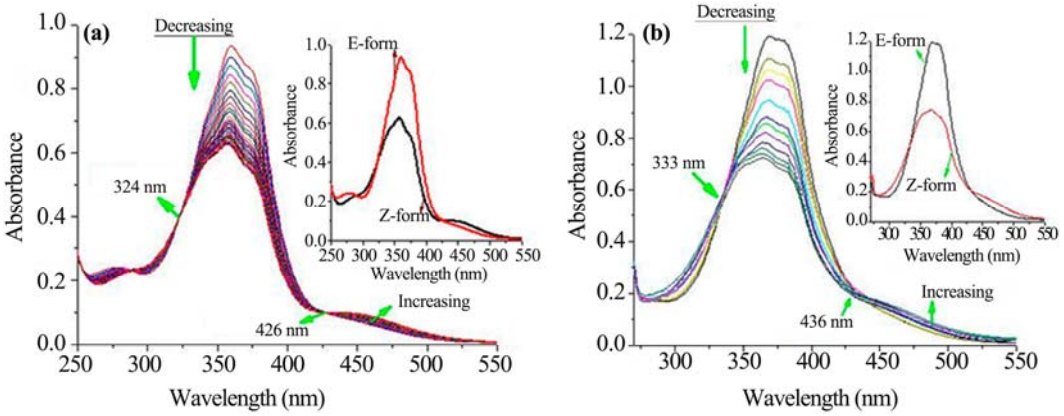

Fig. 2 — (a) Spectral changes of $[Ag(Meaai\text{-}Me)_2](NO_3)$ in MeOH and (b) MeOH in presence of CTAB (1:1) upon repeated irradiation at 370 nm at 5 min interval at 25 °C; Inset: Z-form (*cis)* and E-form (*trans)* isomer of the complex.

Table 1 — Results of photochromism, rate of conversion and quantum yields upon UV light irradiation in presence of different micelle

compounds	Excitation wavelength (nm)♣	Isobestics (nm) ♣	Rate of E→Z conversion x $10^8(s^{-1})$	Quantum Yield E-to-Z
		No micelle		
$[Cu(HaaiMe)_2]ClO_4$ (**1a**)	366	333,448	2.531	0.121
$[Cu(MeaaiMe)_2]ClO_4$ (**1b**)	367	330,449	1.932	0.092
$[Cu(HaaiEt)_2]ClO_4$(**2a**)	368	334,452	2.333	0.112
$[Cu(MeaaiEt)_2]ClO_4$(**2b**)	367	331,447	1.483	0.073
$[Ag(HaaiMe)_2]NO_3$(**3a**)	360	324,426	3.882	0.181
$[Ag(MeaaiMe)_2]NO_3$(**3b**)	363	325,428	3.201	0.152
$[Ag(HaaiEt)_2]NO_3$(**4a**)	361	323,425	3.372	0.163
$[Ag(MeaaiEt)_2]NO_3$(**4b**)	362	326,428	3.021	0.141
		CTAB		
$[Cu(HaaiMe)_2]ClO_4$ (**1a**)	376	340,481	5.494	0.252
$[Cu(MeaaiMe)_2]ClO_4$ (**1b**)	378	342,484	4.863	0.231
$[Cu(HaaiEt)_2]ClO_4$ (**2a**)	377	343,480	4.332	0.203
$[Cu(MeaaiEt)_2]ClO_4$ (**2b**)	375	342,482	4.011	0.192
$[Ag(HaaiMe)_2]NO_3$ (**3a**)	369	333,436	6.283	0.302
$[Ag(MeaaiMe)_2]NO_3$ (**3b**)	370	334,437	5.571	0.271
$[Ag(HaaiEt)_2]NO_3$ (**4a**)	368	3303,438	5.332	0.263
$[Ag(MeaaiEt)_2]NO_3$ (**4b**)	369	332,435	5.111	0.242
		Triton X 100		
$[Cu(HaaiMe)_2]ClO_4$ (**1a**)	374	334,449	4.222	0.202
$[Cu(MeaaiMe)_2]ClO_4$ (**1b**)	376	331,451	3.413	0.163
$[Cu(HaaiEt)_2]ClO_4$ (**2a**)	374	333,452	4.041	0.194
$[Cu(MeaaiEt)_2]ClO_4$ (**2b**)	376	332,448	3.221	0.151
$[Ag(HaaiMe)_2]NO_3$ (**3a**)	368	323,428	5.583	0.243
$[Ag(MeaaiMe)_2]NO_3$ (**3b**)	371	327,429	5.231	0.234
$[Ag(HaaiEt)_2]NO_3$ (**4a**)	365	322,426	4.972	0.196
$[Ag(MeaaiEt)_2]NO_3$ (**4b**)	367	327,429	4.081	0.137
		SDS		
$[Cu(HaaiMe)_2]ClO_4$ (**1a**)	365	330,445	1.433	0.073
$[Cu(MeaaiMe)_2]ClO_4$ (**1b**)	368	328,443	1.062	0.054
$[Cu(HaaiEt)_2]ClO_4$ (**2a**)	365	331,450	1.292	0.066
$[Cu(MeaaiEt)_2]ClO_4$ (**2b**)	364	329,444	0.651	0.032
$[Ag(HaaiMe)_2]NO_3$ (**3a**)	361	322,427	2.763	0.131
$[Ag(MeaaiMe)_2]NO_3$ (**3b**)	362	323,429	1.971	0.094
$[Ag(HaaiEt)_2]NO_3$ (**4a**)	360	321,423	2.322	0.112
$[Ag(MeaaiEt)_2]NO_3$ (**4b**)	363	325,424	1.741	0.082

♣ Data collected from UV-visible absorption spectral studies

of the molecule reduces the rate of isomerisation, *trans*-to-*cis* (Table 1).

Both covalent and noncovalent interactions about the photochrome regulate activity towards stimulation by light. Micelles have both hydrophilic and hydrophobic ends. Above critical micelle concentration (CMC) the molecules are aggregated to generate an organized system. Photochromic molecules may be encapsulated in the hydrophobic phase of the micelle and may influence the alteration of the potential energy of the photochrome (Scheme 3). The analyte in micelle phase becomes more sensitive to physical world which may be due to decrease in molecular association that is practicable among the similar species in bulk[33-35].

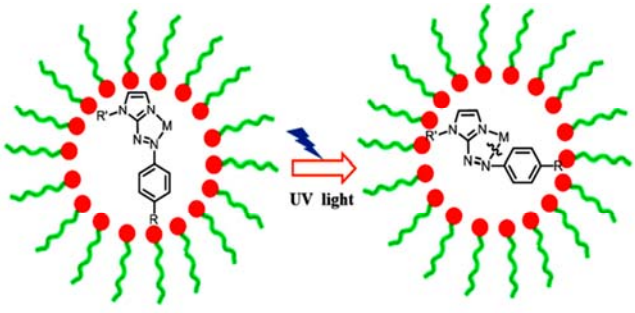

Possible pathway of photochromic movement:
(I) photochrome in core phase; (II) photoisomerisation, trans-to-cis.
Scheme 3

Upon irradiation of UV light to photochrome at the pseudo-phase (in presence of organized media in the solution) the spectra of complexes are recorded and the rate of photoisomerisation are given in Table 1 and Figs 1 and 2. Both static and dynamic phase transformation may be possible in the micelle media of the photochrome. However, static phase is dominating as the micelle forms organized encapsulated state with $[M(RaaiR')_2]ClO_4$. Micelles intensely affect the ground and excited state of the photoactive molecules[34]. In the present study cetyltrimethylammonium bromide (CTAB), Triton-X-100 and sodium dodecyl sulphate (SDS) micelles have been selected as representative of positive, neutral and negative surfaces, respectively. The π-π* transition of photochrome has been shifted to longer wavelength for CTAB and Trito-X100 (Δλ = 3–15 nm) while in case of SDS a small amount of negative shifting is observed. The neutral (Triton-X-100) and cationic micelles (CTAB) enhance the rate of *trans*-to-*cis* isomerisation by 30–70% while anion micelle (SDS) reduces the photoisomerisation rate by 34–49% compare to the no micelle environment (Table 1). The results imply that *cis* configuration in micelle phase is more stable than no-micelle environment with respect to light irradiation[36-38].

Micelles are soft materials and have confined spaces like liquid crystals, gels and polymers[39]. The reaction of a guest molecule in confined spaces could be visualized to occur within a 'reaction cavity' with a defined boundary. The reaction in micelle phase depends on space in the cavity and flexibility of the boundary and weak interactions that hold the guest within the cavity. Among the various weak interactions between the host and guest, hydrophobic, van der Walls and C–H---π are important in the context of the photoreaction of the molecules. Free space surrounding the guest within a restricted space plays a critical role in controlling the motional performance of the species in a confined space[40].

The extent of *trans*-to-*cis* photoisomerisation under UV-irradiation has been controlled by the compartmentalization of the chromophore in the host. Micelle probe is hydrophobic and reduces the noncovalent (C-H--π, π--π) interactions which leads to stabilize the entrapped photochrome[41]. It may be the reason for increased rate of *trans*-to-*cis* photoisomerisation in neutral (Triton-X-100) and cationic (CTAB) micelles than that of free ligand (Table 1). Anion micelle (SDS) may destabilize the *cis*-structure because of strong dipolar interaction than that of *trans*-structure since higher dipole moment of earlier one. This may be the reason for lowering of the rate of photoisomerisation.

Thermal isomerisation, *cis* → *trans*

The irradiation at ~360 nm to the solution of Cu and Ag complexes of 1-alkyl-2-(arylazo)imidazoles in methanol in presence of Trriton-X-100, CTAB and SDS has transformed *trans*-to-*cis*-isomer (>95%) and the same solution has been exposed to the visible light irradiation at 455 nm to transform them to *trans*-isomer. The process is very slow. While the thermal change at dark is relatively fast and the reaction rate is characterized by a single exponential function. The unimolecular rate constant of the thermal backward isomerisation (k) was obtained by the analysis of the measured absorbance:

$$\text{Abs}(t),\ \text{Abs}(t) = (\text{Abs}_t - \text{Abs}_c)e^{-kt} + \text{Abs}_c \qquad \ldots(2)$$

Where Abs_c and Abs_t are absorbances corresponding to pure samples of c (*cis*) and t (*trans*) forms, respectively. The thermal *cis*-to-*trans* isomerisation rates were obtained by monitoring absorption changes intermittently for a *cis*-rich solution kept in the dark at constant temperature (T) in the range 298-313 K. The activation energy (E_a) and the frequency factor (A) were obtained from:

$$\ln k = \ln A - E_a/RT \qquad \ldots (3)$$

Where k is the measured rate constant, R is the gas constant, and T is temperature. The values of the activation free energy (ΔG*) and the activation entropy (ΔS*) were obtained through the relationships:

$$\Delta G^* = E_a - RT - T\Delta S^* \qquad \ldots (4)$$

$$\Delta S^* = \ln A - 1 - \ln(k_B T/h)/R \qquad \ldots (5)$$

Where k_B and *h* are Boltzmann's and Plank's constants, respectively.

The activation energy (E_a) of thermal isomerisation was determined by fitting the temperature dependent k values (Fig. 3) and the results are listed in Table 2. Data reveal that E_a value increases in the micelle phase and the thermal *cis*-to-*trans* isomerisation rate of the ligands are decreased by 20–40% irrespective of nature of micelles. *Cis*-isomer is more polar than *trans*-1-alkyl-2-(arylazo)imidazole. Hence the *cis*-isomer is better stabilized in micelle phase and the thermal data support, indeed (Table 2). A cartoon

Table 2 — Rate and activation parameters for *cis* (c) → *trans* (t) thermal isomerisation

Complexes	Temp (K)	Rate of thermal c→ t conversion x 10^5 (s^{-1})	E_a, kJ mol^{-1}	ΔH^* kJ mol^{-1}	ΔS^* J mol^{-1} K^{-1}	ΔG^{*} [c] kJ mol^{-1}
		No micelle				
$[Cu(HaaiMe)_2]ClO_4$	298	1.6382	43.50	40.09	–183.26	96.90
(**1a**)	303	1.9032				
	308	2.6631				
	313	3.7432				
$[Cu(MeaaiMe)_2]ClO_4$	298	1.7892	42.90	40.37	–181.30	95.75
(**1b**)	303	2.3341				
	308	2.8794				
	313	3.8321				
$[Cu(HaaiEt)_2]ClO_4$	298	1.4491	42.18	39.65	–185.46	96.30
(**2a**)	303	1.8952				
	308	2.3530				
	313	3.3421				
$[Cu(MeaaiEt)_2]ClO_4$	298	1.7772	40.52	37.98	–189.63	95.91
(**2b**)	303	2.1032				
	308	2.7861				
	311	3.8732				
$[Ag(HaaiMe)_2]NO_3$	298	1.3297	56.41	53.87	–137.76	95.95
(**3a**)	303	2.2465				
	308	3.1642				
	313	3.9751				
$[Ag(MeaaiMe)_2]NO_3$	298	1.3245	55.06	52.51	–142.37	96.00
(**3b**)	303	2.2164				
	308	3.0546				
	313	3.8745				
$[Ag(HaaiEt)_2]NO_3$	298	1.3254	53.15	50.61	–148.70	96.03
(**4a**)	303	2.1987				
	308	3.0210				
	313	3.7251				
$[Ag(MeaaiEt)_2]NO_3$	298	1.3191	52.83	50.29	–149.77	96.04
(**4b**)	303	2.2043				
	308	2.9804				
	313	3.7024				
		CTAB				
$[Cu(HaaiMe)_2]ClO_4$	298	1.3364	49.65	47.13	–160.07	96.03
(**1a**)	303	2.3343				
	308	3.0141				
	313	3.5542				
$[Cu(MeaaiMe)_2]ClO_4$	298	1.3371	49.57	47.03	–160.87	96.18
(**1b**)	303	2.0371				
	308	2.7608				
	313	3.5002				
$[Cu(HaaiEt)_2]ClO_4$	298	1.4247	47.98	45.45	–165.38	95.97
(**2a**)	303	2.3019				
	308	3.1142				
	313	3.6003				
$[Cu(MeaaiEt)_2]ClO_4$	298	1.5249	46.88	44.34	–168.87	95.93
(**2b**)	303	2.2099				
	308	3.1002				
	313	3.7242				
$[Ag(HaaiMe)_2]NO_3$	298	1.0658	65.71	63.18	–108.53	96.34
(**3a**)	303	1.8512				
	308	2.6941				
	313	3.8541				

(*Contd.*)

Table 2 — Rate and activation parameters for *cis* (c) → *trans* (t) thermal isomerisation (*Contd*.)

Complexes	Temp (K)	Rate of thermal c→ t conversion x 10^5 (s^{-1})	E_a, kJ mol^{-1}	ΔH^* kJ mol^{-1}	ΔS^* J mol^{-1} K^{-1}	ΔG^{*} [c] kJ mol^{-1}
		CTAB				
$[Ag(MeaaiMe)_2]NO_3$ (**3b**)	298	1.2559	63.81	61.27	–114.23	96.17
	303	1.8132				
	308	2.6571				
	311	4.3651				
$[Ag(HaaiEt)_2]NO_3$ (**4a**)	298	1.1145	63.59	61.05	–115.48	96.33
	303	1.8182				
	308	2.5974				
	313	3.8764				
$[Ag(MeaaiEt)_2]NO_3$ (**4b**)	298	1.2541	61.26	58.71	–122.71	96.20
	303	1.8265				
	308	2.6574				
	313	4.1325				
		TRITON X 100				
$[Cu(HaaiMe)_2]ClO_4$ (**1a**)	298	1.4453	49.15	46.61	–162.53	96.26
	303	1.7052				
	308	2.5330				
	313	3.6521				
$[Cu(MeaaiMe)_2]ClO_4$ (**1b**)	298	1.4326	48.38	45.84	–165.16	96.29
	303	1.6952				
	308	2.5323				
	313	3.5522				
$[Cu(HaaiEt)_2]ClO_4$ (**2a**)	298	1.4002	47.67	45.13	–167.42	96.27
	303	1.8342				
	308	2.5431				
	313	3.5002				
$[Cu(MeaaiEt)_2]ClO_4$ (**2b**)	298	1.4021	45.54	43.00	–174.50	96.30
	303	1.8732				
	308	2.3541				
	313	3.4621				
$[Ag(HaaiMe)_2]NO_3$ (**3a**)	298	1.1241	54.27	51.74	–147.29	96.74
	303	1.4321				
	308	2.1570				
	313	3.1542				
$[Ag(MeaaiMe)_2]NO_3$ (**3b**)	298	1.1021	52.67	50.13	–152.77	96.80
	303	1.3941				
	308	2.1578				
	313	2.9587				
$[Ag(HaaiEt)_2]NO_3$ (**4a**)	298	1.0001	58.49	55.95	–134.22	96.95
	303	1.2357				
	308	2.0941				
	313	2.9541				
$[Ag(MeaaiEt)_2]NO_3$ (**4b**)	298	0.9001	57.11	54.57	–139.30	97.13
	303	1.2421				
	308	2.0104				
	313	2.6151				
		$[Cu(HaaiMe)_2]ClO_4$ (**1a**)				
$[Cu(MeaaiMe)_2]ClO_4$ (**1b**)	298	1.7312	34.20	31.65	–210.60	95.98
	303	2.2160				
	308	2.7811				
	313	3.3452				
$[Cu(HaaiEt)_2]ClO_4$ (**2a**)	298	1.8102	33.21	30.67	–213.62	95.93
	303	2.3132				
	308	2.6563				
	313	3.5313				

(*Contd*.)

Table 2 — Rate and activation parameters for *cis* (c) → *trans* (t) thermal isomerisation (*Contd*.)

Complexes	Temp (K)	Rate of thermal c→ t conversion x 10^5 (s^{-1})	E_a, kJ mol^{-1}	ΔH^* kJ mol^{-1}	ΔS^* J mol^{-1} K^{-1}	ΔG^{*} [c] kJ mol^{-1}
		$[Cu(HaaiMe)_2]ClO_4$ (**1a**)				
$[Cu(MeaaiEt)_2]ClO_4$ (**2b**)	298	1.7812	32.42	29.89	–216.46	96.02
	303	2.2003				
	308	2.6810				
	313	3.3479				
$[Ag(HaaiMe)_2]NO_3$ (**3a**)	298	1.7902	26.36	23.81	–236.42	96.03
	303	2.3124				
	308	2.6653				
	313	3.0042				
$[Ag(MeaaiMe)_2]NO_3$ (**3b**)	298	1.4102	45.96	43.43	–173.05	96.30
	303	1.8561				
	308	2.4310				
	313	3.4651				
$[Ag(HaaiEt)_2]NO_3$ (**4a**)	298	1.4124	43.86	41.32	–180.07	96.33
	303	1.8657				
	308	2.3341				
	313	3.3684				
$[Ag(MeaaiEt)_2]NO_3$ (**4b**)	298	1.4321	42.77	40.23	–183.64	96.32
	303	1.8642				
	308	2.3157				
	313	3.3451				
$[Cu(HaaiMe)_2]ClO_4$ (**1a**)	298	1.4531	42.09	39.54	–185.85	96.31
	303	1.8762				
	308	2.3315				
	313	3.3651				

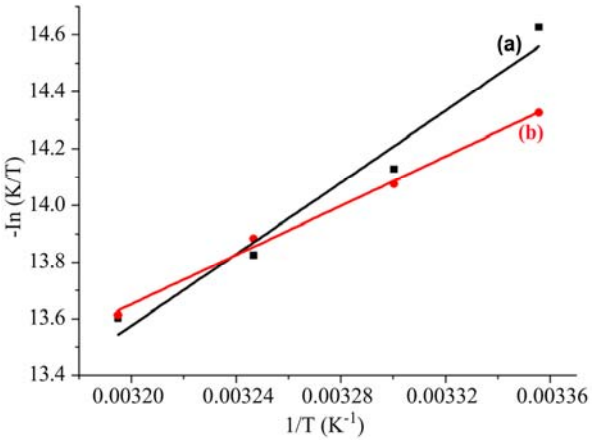

Fig. 3 — The Eyring plots of rate constants of *cis*-to-*trans* thermal isomerisation of (a) $[Cu(MeaaiMe)_2]ClO_4$(**1b**) and (b) $[Ag(MeaaiMe)_2]ClO_4$(**3b**)) Triton-X-100.

in Scheme 3 explains the plausible mechanism of photoisomerisation of coordinated 1-alkyl-2-(arylazo) imidazole in micelle media.

Theoretical Computation

Optimized structures of $[Cu(MeaaiMe)_2]^+$ (**1b**) and $[Ag(MeaaiMe)_2]^+$ (**3b**) have been generated from DFT computations and the electronic configuration, spectral transitions are validated from the calculation of molecular functions. The optimized structures and some notable bond parameters are added in Fig. 4. The bond parameters of the calculated structures are closer to the previously determined single crystal X-ray structures of the complexes; the X-ray structure[42] of $[Ag(Haai\text{-}C_{22}H_{45})_2]^+$ shows Ag-N(imidazolyl), 2.146(4); Ag-N(azo), 2.650(4); N=N, 1.273(5) Å and N(imidazolyl)-Ag-N(azo), 67.44(12)°. Similarly, $[Cu(HaaiMe)_2]^+$ determines the bond parameters[32] as Cu-N(imidazolyl), 2.006(3); Cu-N(azo), 2.026(3); N=N, 1.281(4) Å and N(imidazolyl)-Cu-N(azo), 80.6(1)°. The theoretical N=N, M-N(azo), M(imidazolyl) distances and the chelate angle, N(azo)-M-N(imidazolyl) are longer than reported structures.

The surface plots of the MOs along with their energy and composition are given in Fig. 5. Data reveal that both occupied and vacant MOs in these two series of complexes are dominated by characteristics of ligand features. The optimized structure of the E-isomer is more stable than the Z-isomer by 5765 kcal (250 eV) for $[Cu(MeaaiMe)_2]^+$ (**1b**) and 5696 kcal (246 eV) for $[Ag(MeaaiMe)_2]^+$ (**3b**) complex (Fig. 6). The E-isomer functions are used to interpret spectroscopic results. In $[Cu(MeaaiMe)_2]^+$ (**1b**) the HOMO (–8.76 eV) of the E-isomer is stabilized by 3.27 eV compared to LUMO (–5.49 eV).

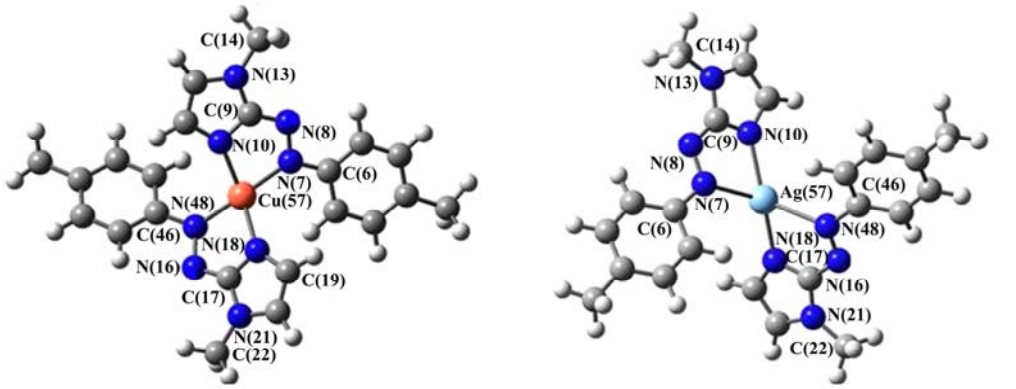

$[Cu(MeaaiMe)_2]^+$ (**1b**)

Cu(57)-N(7), 2.00294; Cu(57)-N(10), 2.06724;

N(7)-N(8), 1.43727 Å; N(7)-Cu(57)-N(10), 81.78502°;

N(7)-Cu(57)-N(18), 81.78502°

$[Ag(MeaaiMe)_2]^+$ (**3b**)

Ag(57)-N(7), 2.44902; Ag(57)-N(10), 2.24662;

N(7)-N(8), 1.38212 Å; N(7)-Ag(57)-N(10), 73.03312°;

N(7)-Ag(57)-N(18), 124.56520°

Fig. 4 — Optimized structures of $[Cu(MeaaiMe)_2]^+$ (**1b**) and $[Ag(MeaaiMe)_2]^+$ (**3b**) drawn by using DFT-B3LYP Function.

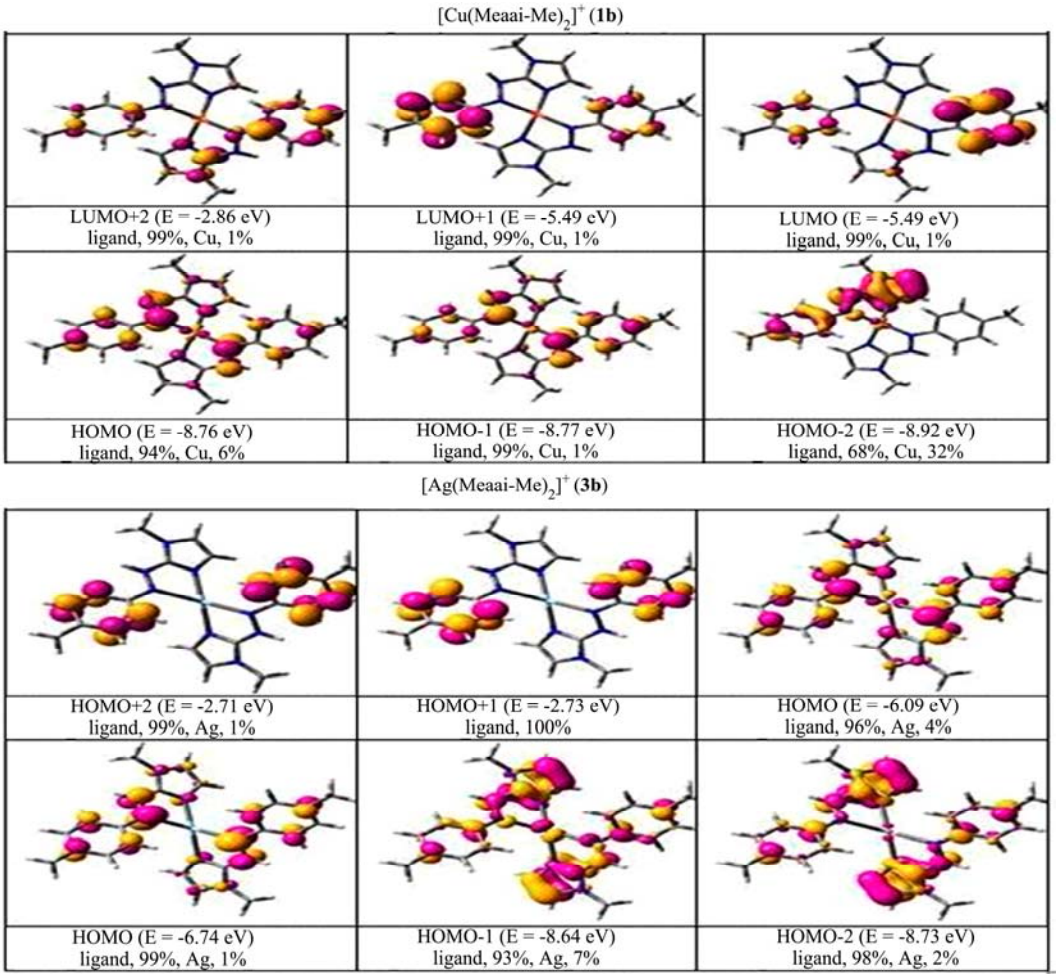

Fig. 5 — Surface plots of some MOs of $[Cu(MeaaiMe)_2]^+$ (**1b**) and $[Ag(MeaaiMe)_2]^+$ (**3b**).

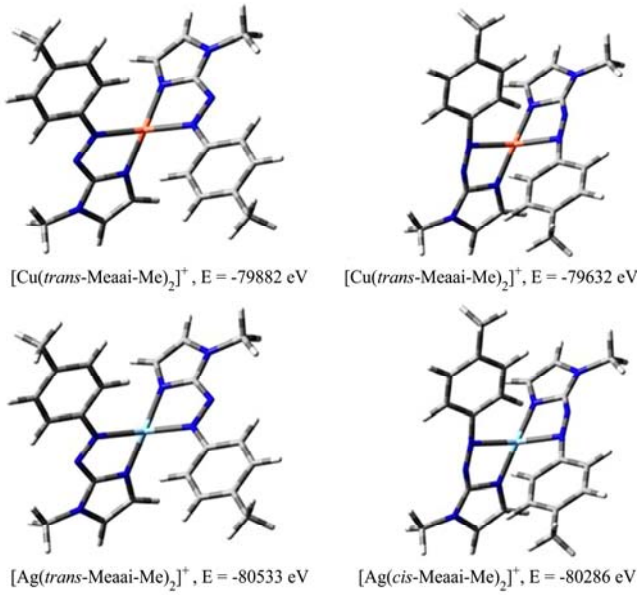

Fig. 6 — Calculated energy of *trans*- and *cis*- isomers of $[M(MeaaiMe)_2]^+$.

High intense bands calculated at 453.84 (oscillator strength f, 0.5616), 360.09 (f, 0.0586), are referred to the HOMO-3→LUMO and HOMO-7→LUMO+2, respectively, and have been assigned mainly to intra-ligand charge transfer (ILCT) bands. In $[Ag(MeaaiMe)_2]^+$ (**3b**) the HOMO (–6.74 eV) and LUMO (–6.09 eV) energy gap is only 0.65 eV. The calculated appreciable transitions appear at 367.65 nm (f, 0.0465) and 316.24 nm (f, 0.2201) and are assigned to ILCT bands.

Upon UV light irradiation the more stable *trans*-isomer (E) isomerizes to the *cis*-isomer (Z). This is due to π-π* transition which causes cleavage of the M–N(azo) bond and opening of the chelate ring, followed by the isomerization to *cis*-structure. Besides, the metal-complex promotes other charge transition such as, LMCT or CRCT (chain-to-ring CT) processes, which may be liable for deactivation of the excited species and regulates the rate of isomerization and quantum yields

Conclusions

$[M(RaaiR')_2]ClO_4$ [M = Cu(I), Ag(I); RaaiR' = 1-Alkyl-2-(arylazo)imidazole] serve as photochromic complexes. The coordinated RaaiR' carries pendant –N=N-Ar group and undergoes light induced *trans*-to-*cis* isomerization. Effect of micelle (SDS, CTAB, Triton-X-100) on the rates and quantum yield of photoisomerization is examined. The rate of photoisomerisation, *trans*-to-*cis* increases with the addition of neutral (Triton-X-100) and cation (CTAB) micelles while the rate decreases in presence of anion micelle (SDS).

Supplementary Data

Supplementary data associated with this article are available in the electronic form at: http://nopr.niscair.res.in/jinfo/ijca/IJCA_59A(02)189-199_SupplData.pdf.

References

1 Balzani V, Venturi M & Credi A, *Molecular Devices and Machines: Concepts and Perspectives for the Nanoworld*, (Wiley-VCH:Weinheim Germany) 2008.
2 Kay E R & Leigh D A, *Angew Chem Int Ed Engl*, 54 (2015) 10080.
3 Sato O, Tao J & Zhang Y-Z, *Angew Chem Int Ed*, 46 (2007) 2152.
4 Karimi M, Ghasemi A, Zangabad P S, Rahighi R ,Basri S M M, Mirshekari H, Amiri M, Pishabad Z S, Aslani A, Bozorgomid M, Ghosh D, Beyzavi A, Vaseghi A, Aref A R, Haghani L, Bahrami S & Hamblin M R, *Chem Soc Rev*, 45(5) (2016) 1457.
5 Nicoletta F P, Cupelli D, Formoso P, Filpo G D, Colella V & Gugliuzza A, *Membranes,* 2 (2012) 134.
6 Hartley G S, *Nature*, 140 (1937) 281.
7 Durr H & Laurent H B, *Photochromism: molecules and systems*, (Elsevier, Amsterdam) 2003.
8 Feringa B, *Molecular switches*, (Wiley-VCH) 2001.
9 Beharry A A & Woolley G A, *Chem Soc Rev*, 40 (2011) 4422.
10 Otsuki J, Suwa K, Narutaki K, Sinha C, Yoshikawa I & Araki K, *J Phys Chem A,* 109 (2005) 8064.
11 Otsuki J, Suwa K, Sarker K K & Sinha C, *J Phys Chem A,* 111 (2007) 1403.
12 Sarker K K, Halder S S, Banerjee D, Mondal T K, Paital A R, Nanda P K, Raghavaiah P & Sinha C, *Inorg Chim Acta,* 363 (2010) 2955.
13 Sarker K K, Sardar D, Suwa K, Otsuki J & Sinha C, *Inorg Chem*, 46 (2007) 8291.
14 Sarker K K, Chand B G, Suwa K, Cheng J, Lu T -H, Otsuki J & Sinha C, *Inorg Chem*, 46 (2007) 670.
15 Pratihar P, Mondal T K, Patra A K & Sinha C, *Inorg Chem,* 48 (2009) 2760.
16 Saha G, Datta P, Sarkar K K, Saha R , Mostafa G & Sinha C, *Polyhedron*, 30 (2011) 614.
17 Mallick D, Nandi A, Datta S, Sarker K K, Mondal T K & Sinha C, *Polyhedron,* 31 (2012) 506.
18 Schultz T, Quenneville J, Levine B, Toniolo A, Martı´nez T J, Lochbrunner S, Schmitt M, Shaffer J P, Zgierski M Z & Stolow A, *J Am Chem Soc,* 125 (2003) 8098.
19 Chantrapromma S, Fun H –K & Sinha C, *Polyhedron,* 22 (2003) 247.
20 Nandi A, Sen C, Roy S, Mallick D, Sinha R, Mondal T K & Sinha C, *Polyhedron,* 79 (2014) 186.
21 Lee C, Yang W & Parr R G, *Phys Rev B*, 37 (1988) 785.
22 Gaussian 03, Revision D.01, Frisch M J, Trucks G W, Schlegel H B, Scuseria G E, Robb M A, Cheeseman J R, Jr. Montgomery J A, Vreven T, Kudin K N, Burant J C, Millam J M, Iyengar S S, Tomasi J, Barone V, Mennucci B,

Cossi M, Scalmani G, Rega N, Petersson G A, Nakatsuji H, Hada M, Ehara M, Toyota K, Fukuda R, Hasegawa J, Ishida M, Nakajima T, Honda Y, Kitao O, Nakai H, Klene M, Li X, Knox J E, Hratchian H P, Cross J B, Bakken V, Adamo C, Jaramillo J, Gomperts R, Stratmann R E, Yazyev O, Austin A J, Cammi R, Pomelli C, Ochterski J W, Ayala P Y, Morokuma K, Voth G A, Salvador P, Dannenberg J J, Zakrzewski V G, Dapprich S, Danie A D, Strain M C, Farkas O, Malick D K, Rabuck A D, Raghavachari K, Foresman J B , Ortiz J V, Cui Q, Baboul A G, Clifford S, Cioslowski J, Stefanov B B, Liu G, Liashenko, Piskorz A P, Komaromi I, Martin R L, Fox D J, Keith T, Al-Laham M A, Peng C Y, Nanayakkara A, Challacombe M, Gill P M W, Johnson B, Chen W, Wong M W, Gonzalez C & Pople J A, Gaussian, Inc., Wallingford C T, 26, (2004)

23 GaussView3.0, Gaussian: Pittsburgh, P A.

24 Hay P J & Wadt W R, *J Chem Phys*, 82 (1985) 270.

25 Bauernschmitt R & Ahlrichs R, *Chem Phys Lett*, 256 (1996) 454.

26 Casida M E, Jamorski C, Casida K C & Salahub D R, *J Chem Phys*, 108 (1998) 4439.

27 Stratmann R E, Scuseria G E & Frisch M J, *J Chem Phys*, 109 (1998) 8218.

28 Cossi M, Rega N, Scalmani G & Barone V, *J Comput Chem*, 24 (2003) 669.

29 O'Boyle N M, Tenderholt A L & Langner K M, *J Comput Chem*, 29 (2008) 839.

30 Senapoti S, Sarker K K, Mondal T K & Sinha C, *Transition Met Chem,* 31 (2006)293.

31 Misra T K, Das D & Sinha C, *Polyhedron,* 16 (1997) 4163.

32 Dinda J, Ray U, Mostafa G, Lu T H, Usman A, Razak I A, Chantraprumma S, Fun H K & Sinha C, *Polyhedron*, 22 (2003) 247

33 Zimmerman G, Chow L & Paik U, *J Am Chem Soc,* 80 (1958) 3528.

34 Schwemer J, Pepe I M, Paulsen R & Cugnoli C, *J Comp Physiol A*, 154 (1984) 549.

35 Hayase K, Hayano S, *J Colloid Interface Sci,* 63 (1978) 446.

36 Serra F & Terentjev E M, *Macromolecules,* 41 (2008) 981.

37 Zio´łek M & I Sobczak A E I, *J Incl Phenom Macrocycl Chem*, 63 (2009) 211.

38 Crano J C & R. J. Guglielmetti R J, *Organic Photochromic and Thermochromic Compounds: Physicochemical studies,* (Springer), 1999.

39 Kok J D, *Photochem Photobiol*, 42 (1985) 663.

40 Mata J, Patel J, Jain N, Ghosh G & Bahadur P, *J Colloif Interface Sci,* 297 (2006) 797.

41 Parthasarathy A & Ramamurthy V, *Photochem Photobiol Sci,* 10 (2011) 1455.

42 Sakai H, Ebana H, Sakai K, Tsuchiya K, Ohkubo T & Abe M, *J Colloid Interface Sci,* 316 (2007) 1027.